



**Universidade de São Paulo**

**Biblioteca Digital da Produção Intelectual - BDPI**

---

Departamento de Mecânica - EP/PME

Artigos e Materiais de Revistas Científicas - EP/PME

---

2013-01-30

# Relation between magnetic Barkhausen noise and hardness for jominy quench tests in SAE 4140 and 6150 steels

---

<http://www.producao.usp.br/handle/BDPI/46487>

*Downloaded from: Biblioteca Digital da Produção Intelectual - BDPI, Universidade de São Paulo*

# Relation Between Magnetic Barkhausen Noise and Hardness for Jominy Quench Tests in SAE 4140 and 6150 Steels

Freddy A. Franco · M.F.R. González · M.F. de Campos · L.R. Padovese

Received: 16 March 2012 / Accepted: 30 October 2012 / Published online: 18 November 2012  
© Springer Science+Business Media New York 2012

**Abstract** The nondestructive Magnetic Barkhausen Noise (MBN) technique was applied for the evaluation of SAE 4140 and SAE 6150 steels after a Jominy end-quench test. Microstructures were also characterized by SEM (Scanning Electron Microscope) and hardness tests. MBN measurements were performed on the same sample regions at three excitation frequencies. Different parameters of the measured signals (signal peak position and height, and Root mean square) were calculated. A relationship between mechanical hardness and MBN parameters was found for both materials, with the best correlation coefficient being found in low excitation frequency range.

**Keywords** Barkhausen noise · Hardness measurement · Microstructure · Magnetic non-destructive testing

---

F.A. Franco (✉)  
Sociedade Educacional de Santa Catarina, Mestrado em Engenharia Mecânica, Rua Albano Schmidt, 3333, Joinville, SC 89.206-001, Brazil  
e-mail: [freffranco@gmail.com](mailto:freffranco@gmail.com)

M.F. González  
Department of Metallurgical and Materials Engineering, Engineering School, University of São Paulo, SP, Av. Prof. Mello Moraes, 2463, 05508-030 São Paulo, Brazil

M.F. de Campos  
EEIMVR—Universidade Federal Fluminense, Av dos Trabalhadores 420 Vila Santa Cecília, Volta Redonda, RJ 27255-125, Brazil

L.R. Padovese  
Department of Mechanical Engineering, Engineering School, University of São Paulo, SP, Av. Prof. Mello Moraes, 2231, 05508-900 São Paulo, Brazil

## 1 Introduction

A Jominy test is a typical hardenability test for steels. A Jominy test predicts the hardenability using hardness measurements in a quenched bar as a basis, and is a simple and practical test [1]. However, the Jominy test requires the measurement of hardness, and this is time consuming and expensive. The Jominy test is very relevant for industry [2] and there is research aiming the theoretical prediction of hardness at different points of the Jominy bar [3]. The verification of these models request hardness measurements. Neural networks have been used for the extrapolation of Jominy test data [4]. Frequently, data from the Jominy test are extrapolated to true pieces. The measurement of hardness in the produced piece is useful for quality control, but this may not be feasible. There are problems, like the complicated geometry of the sample not allowing a hardness measurement in hardness machines. Besides, hardness tests are somewhat destructive, producing an impression in the specimen for each measurement.

Thus, it is of great interest that an alternative method be found for the hardness measurements. This can be achieved with the nondestructive Magnetic Barkhausen Noise (MBN) Test, as discussed further in this study. MBN is very rapid, easy and practical, allowing an estimate of the hardness even in the production line.

For steels, there is a relationship between mechanical and magnetic properties. Already in the XIX century, it was discovered that hard steels also present a large hysteresis area, and that soft steels, on the other hand, present a small hysteresis area. This is the origin of the names hard magnetic materials and soft magnetic materials [5]. Magnetically soft steels have this name because they can be easily magnetized, and this happens due to the free movement of the domain walls. However, magnetically hard steels have crystalline defects, which make difficult the domain wall moving.

The analogy between hard and soft (for both mechanical and magnetic behavior) is because of the crystalline defects. The same defects that usually produce pinning of dislocations—and increase hardness—also produce pinning of domain walls. However, dislocations are linear defects (1D—one-dimensional) of only 5 Angstroms (thickness), and domain walls are in fact 3D (three-dimensional) defects, with thickness of  $\sim 1000$  Angstroms for iron and steels. Thus, for example, a puncture defect as a vacancy may pin a dislocation, but it cannot pin a domain wall. But many defects, such as grain boundaries, interfaces, inclusions and dislocation cells, can stop both dislocations and domain walls, and this phenomenon thus increases both the magnetic and mechanical hardness.

Soft magnetic materials have high magnetic permeability, and this happens because the domain walls can move easily. In the case of heat treated and quenched steels, there has been found a connection between initial permeability and RMS (root mean square) of MBN [6]. The same relation can be used to estimate mechanical hardness.

Inside ferromagnetic materials there is a random distribution of magnetic domains in which magnetic moments are aligned normal to the axis of easy magnetization of the crystalline structure. When these materials are subjected to a variable magnetic field, the size and direction of magnetic domains change due to domain wall movements. Barkhausen [7] reported that the domain wall movement produces a noise, which can be detected as a voltage pulse induced in a pickup winding coil placed around the material sample or on its surface. This noise is the so-called magnetic Barkhausen noise (MBN).

Martensite is very hard because many crystalline defects appear when the transformation of austenite to martensite takes place. These defects may stop the movement of either dislocations or domain walls. The martensite transformation leads to (i) a large number of interfaces, (ii) carbon in solid solution generating stress in the lattice, (iii) a high density of dislocations [8].

Products of the decomposition of the austenite show increasing hardness with increasing cooling speed after austenitization, as seen in the CCC (Continuous-Cooling-Curves) [9]. The following hardness relationship can be observed:

Martensite > bainite > pearlite > ferrite

Bainite is a constituent with large number of interfaces, and with hardness intermediate between martensite and pearlite. In general, when the steel microstructure is finer, the harder is the material, because the interfaces act as obstacles for dislocations. If the grain size is very small, in the nanocrystalline size, another mechanism for magnetization reversal can happen: domain rotation [8]. The Barkhausen noise

emission is smaller for domain rotation rather than for domain wall movement [10]. Several authors [11, 12] have confirmed that plastic deformation, with the consequent presence of dislocations in the lattice, also significant reduces the Barkhausen noise emission [13].

Due to its sensitivity to microstructure variations, the MBN has been used as a nondestructive testing technique (NDT) for ferromagnetic materials in different studies. One interesting application of MBN is for evaluation of residual stresses [14–16]. There are two main types of residual stress, macro-residual stress and micro-residual stress (also called of the first kind and of the third kind residual stress, respectively) [16–18]. The large XRD peak broadening after martensitic transformation suggests significant micro-residual stress, caused by the high density of dislocations and carbon in solid solution [8]. The magnitude of macro-residual stress and micro-residual stress in cold-rolled low carbon steels were compared and it was found that the cold rolling process introduces significant micro residual stress (of the 3rd kind) [18]. For low carbon steels, which are magnetostrictive positive, macro compressive stress (of 1st kind) results in reduction of the MBN, whereas macro tensile stress (of 1st kind) increases the MBN signal [13, 19]. In many cases, the dominant stresses are the micro-residual stress (of the 3rd kind), as previously discussed [8, 18].

MBN measurements have shown high sensitivity and agreement in relation to classic techniques used to measure residual stresses. Meyendorf and Roesner [20] evaluated effects of mechanical hardness and residual stresses by both x-ray diffraction and MBN methods, and found good correlation. Capo-Sanchez et al. [21] found that the magnetic easy axis can be predicted by analyzing the angular distribution of the magnetic Barkhausen noise energy, and the applied uniaxial stress gives origin to a continuous rotation of the magnetic easy axis. In relation to plastic and elastic deformation effects, Stefanita et al. [22] have shown that MBN initially increases with elastic stress and then decreases at very high plastic stress levels, and that elastic effects are far more significant. Alberteris Campos et al. [23] indicated that the magnetic anisotropy coefficient (based on MBN) can be used to characterize the linear and nonlinear elastic limits of the material under tensile stresses. MBN is also sensitive to grain size. Anglada-Rivera et al. [24] reported that the amplitude of the MBN voltage decreases with grain size, essentially due to the fact that for fine grain samples, the number of domains walls that can move is much larger than in the samples with coarse grain. Studies of fatigue damage using MBN signals have also been reported by Moorthy et al. [25] and Palma et al. [26].

Several studies have described the use of MBN to characterize steel and cast iron microstructures affected by different heat treatments. For example, Altpeter [27] estimated the amount of cementite in white cast iron by means of MBN.

**Table 1** Chemical composition of the studied materials (wt%)

Steel	C	Mn	Si	P	S	Cr	Ni	Mo	V	Al	Cu	N
SAE-4140	0.390	0.870	0.240	0.021	0.026	0.980	0.020	0.170	–	0.035	0.010	0.005
SAE-6150	0.520	0.820	0.190	0.010	0.007	0.930	0.120	0.020	0.169	–	–	–

Gur and Cam [28] have shown that the magnitude and position of Barkhausen noise peaks are affected by microstructural changes induced during several heat treatments for SAE 1040 and SAE 4140 steels. In another study, Davut and Gur [29] tempered SAE 5140 steel samples for temperatures between 200 °C and 600 °C; the results showed that when quenching temperature increases, the Barkhausen activity also increases due to softening of martensite. Additionally, in studies conducted by Kleber et al. [30], ferrite-martensite steel structures that appear as a consequence of some heat treatments have also been characterized by MBN since the Barkhausen noise easily distinguishes the two phases, ferrite and martensite. Also, magnetic measurements were effectively used by Kaplan et al. [31] for studying microstructural changes in quenched AISI 8620 steel specimens. Summarizing, there is a clear trend indicating that when martensite volume fraction increases the MBN emission decreases, which should be attributed to occurrence of domain rotation in the martensite [8, 32].

The aim of the present study is to characterize steel microstructures by evaluating, through the Barkhausen method, a continuous microstructure profile change, produced in a single sample by the Jominy end-quench test. The characterization is carried out for two types of structural steels: SAE 4140 and 6150. This provides another example of the versatility of the MBN method.

**2 Material and Methods**

**2.1 Materials**

SAE-4140 and the SAE-6150 steel samples, of chemical composition presented in Table 1, were used in the experimental tests. For both materials, cylindrical samples (25 mm in diameter, and 101.6 mm in length) were manufactured for the Jominy end-quench test according to the ASTM-A225 standard (1999) [33] (for future reference in this paper, the surface in contact with water jet will be called WJ). The studies were carried out in the longitudinal central region of samples, since microstructural variations generated in the longitudinal region were supposed to be more representative than those on the sample surface, due to the fact that the cooling rate was less heterogeneous in this central region. Therefore, after the heat treatment, samples were cut in two halves, along the longitudinal direction. Cuts were

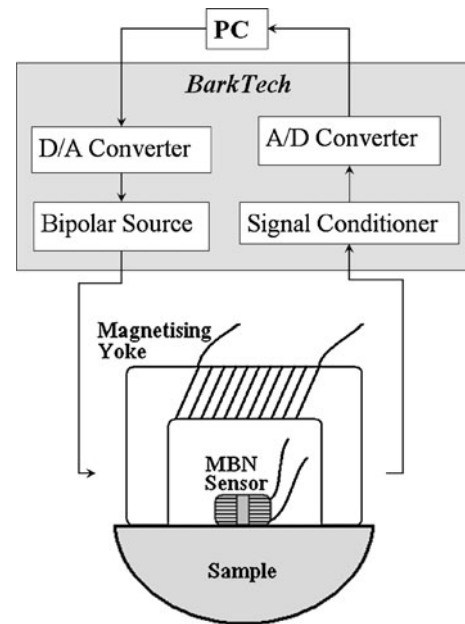


**Fig. 1** Experimental setup

made by an abrasive disk cutting machine under low speed and refrigeration, in order to avoid possible modifications in the sample microstructure. After the cut, the surface layer (1 mm) was removed by polishing.

**2.2 Measuring Techniques**

**2.2.1 Magnetic Barkhausen Noise (MBN)**

MBN measurements were carried out via a piece of portable equipment, named “Barktech”, developed in our laboratory. Figure 1 shows a simplified sketch of this equipment. A sinusoidal wave current was applied to the MBN probe, with 0.8 A amplitude and 5, 10 and 20 Hz frequencies. The MBN signal was measured with a pick-up coil of high sensitivity (with 1000 turns of 0.05 mm diameter wire). The MBN sensor signal was amplified, band pass filtered (1–100 kHz), and sampled at a 200 kHz frequency.

The MBN measurements were made in the central region of a longitudinal flat sample surface at points located at each 1.58 mm on the quenched surface. Each measurement is composed of MBN signals generated in two complete magnetization cycles. Different parameters of measured signals were calculated as the Peak position relative to the applied

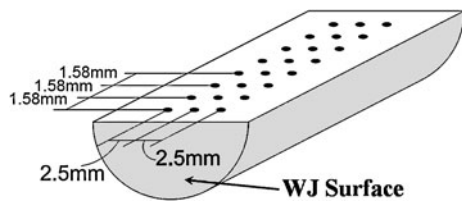


**Fig. 2** Hardness measurement positions in each sample

current and maximum Peak height of signal shape and MB-Nrms. A smoothing by sliding average method was used for obtain MBN signal shape (envelope). Each measurement condition was repeated 10 times.

### 2.2.2 Hardness

Rockwell C (HRC) hardness measurements were obtained by an Otto Wolpert-Werke equipment with a 1471.5 N load. The measurements were made at the same positions as the MBN measurements, i.e., at each 1.58 mm on the quenched surface. For each position (at each 1.58 mm), three hardness measurements were taken. Figure 2 illustrates the sample measuring positions.

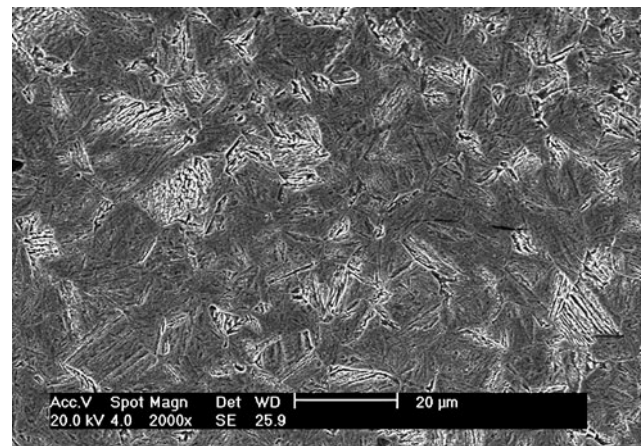
### 2.2.3 Microstructural Analysis

Microstructural analyses were carried out in regions located at different distances from the WJ surface (see Fig. 2). The sample surface was metallographically polished (Fig. 2), removing up to 1 mm depth. Nital at 3 % was used to etch the samples. Sample images were obtained by a Philips Scanning Electron Microscope, model LX30.

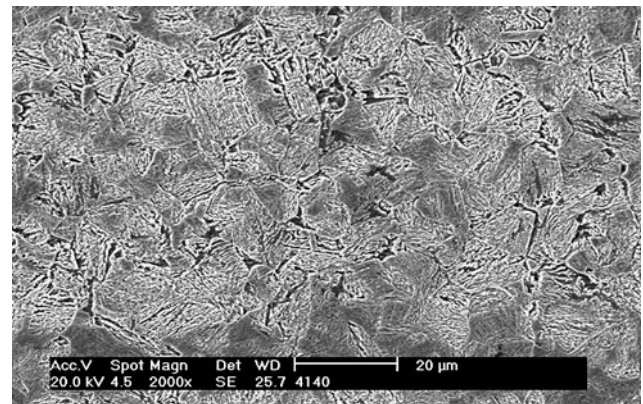
## 3 Results and Discussion

Figures 3 and 4 show the microstructure of SAE-4140 and SAE 6150 steels, respectively. Each photograph represents a specific position with reference to surface WJ. High cooling rates, in regions situated at short distances from the quenched surface, give rise to greater concentration of martensite.

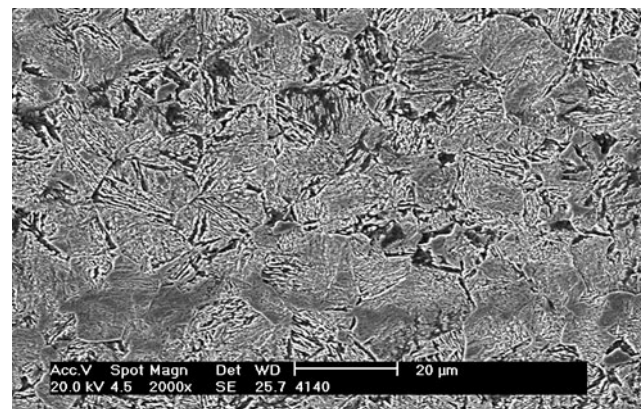
The microstructure of the 4140 steel, at a 11.11 mm distance from the WJ surface, is mainly composed of martensite and bainite. These phases are axially oriented in the sample. Dark areas are identified as martensite (see Fig. 3a), as reported by Gur and Cam [28]. At 19.05 mm distance, a smaller amount of martensite is found, with an increase of bainite amount (Fig. 3b). Due to a lower cooling rate in this region, the transformation tends to produce bainite. As the distance increases to 23.81 mm (Fig. 3c), the microstructure is formed mostly of bainite and other dual phase (ferrite and cementite) constituents resulting from austenite



(a)



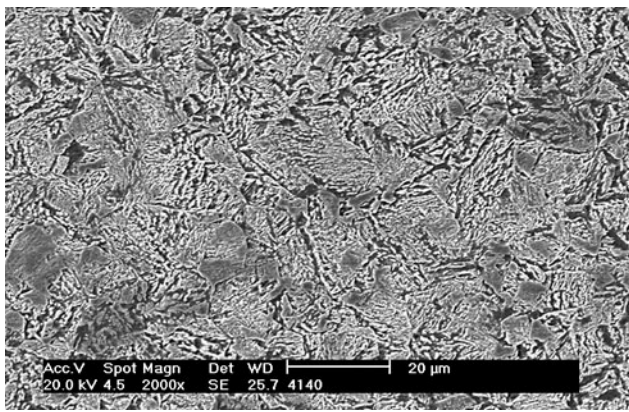
(b)



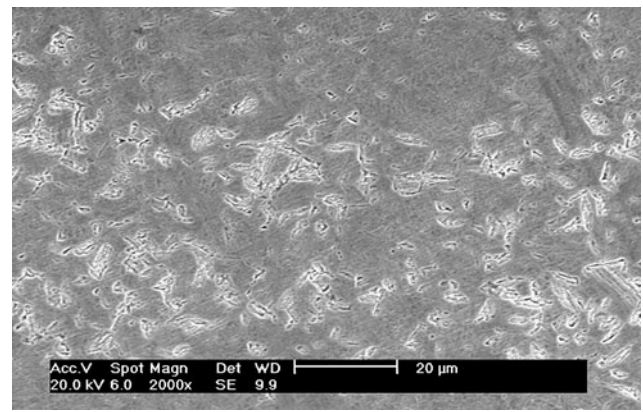
(c)

**Fig. 3** Jominy sample micrographics of SAE-4140 steel for regions located at different distances from the surface WJ; (a) 11.11 mm, 2000X, (b) 19.05 mm, 2000X, (c) 23.81 mm, 2000X, (d) 34.92 mm, 2000X, and (e) 41.27 mm, 2000X

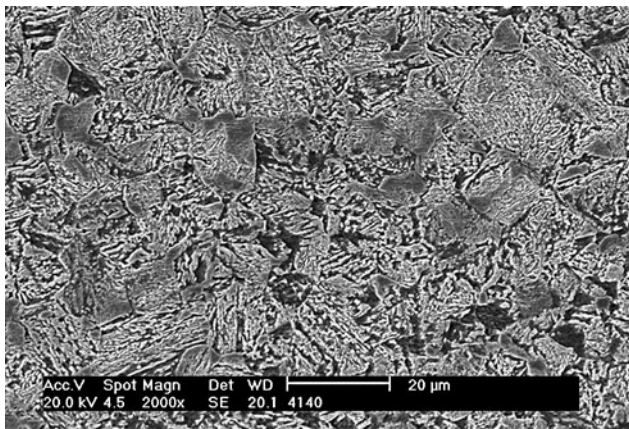
decomposition and less by martensite. The regions at distances of 34.92 mm and 41.27 mm (Figs. 3d and 3e) show less martensite as well as larger amounts of bainite and other constituents resulting from austenite decomposition.



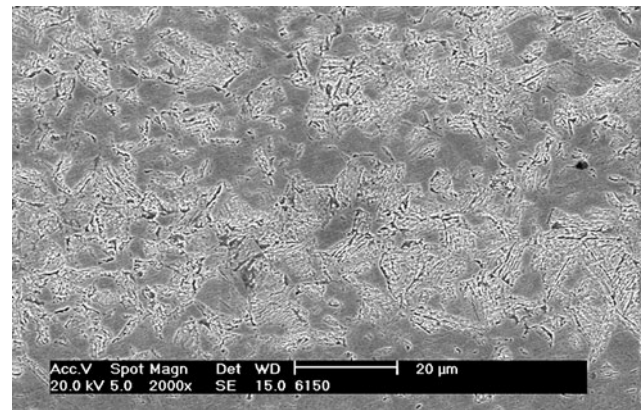
(d)



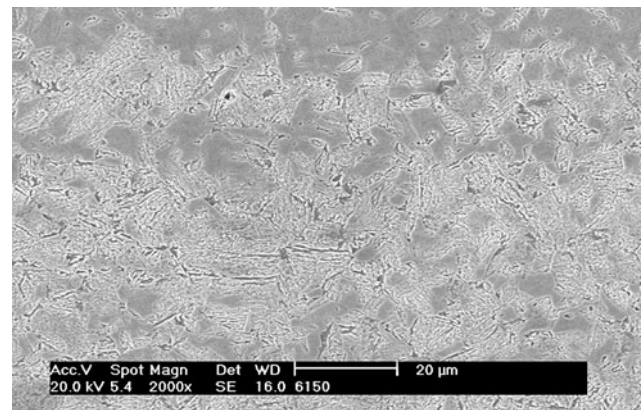
(a)



(e)



(b)



(c)

**Fig. 3** (Continued)

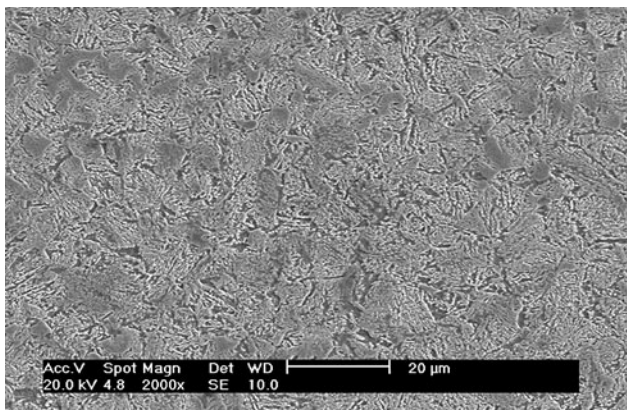
SAE-6150 steel microstructural variations originated by the Jominy test are similar to those related to SAE 4140 steel. For a 11.11 mm distance from WJ surface, the microstructure consists of martensite and bainite (Fig. 4a), with the dark areas ascribed to martensite. As the distance increases to 15.87 mm and 22.22 mm (Figs. 4b and 4c), the smaller cooling rate reduces the martensite amount, but increases the bainite. For a 34.92 mm distance, the microstructure is mainly formed by bainite and other dual phase (ferrite and cementite) constituents resulting from the decomposition of austenite (Fig. 4d). An even larger amount of bainite and others two-phase constituents resulting from the decomposition of austenite was observed for a 41.27 mm distance (Fig. 4e).

In summary, the obtained microstructures—as function of the cooling rate—present similar behaviors for both materials SAE 4140 and SAE 6150. With increasing distance from the quenched surface, martensite percentages are reduced whereas bainite and other coarser constituents resulting from the decomposition of austenite increase. In other words, when cooling rate decreases, the microstructure is coarser, with less crystalline defects, allowing free movement of domain walls. In addition, the nanocrystalline struc-

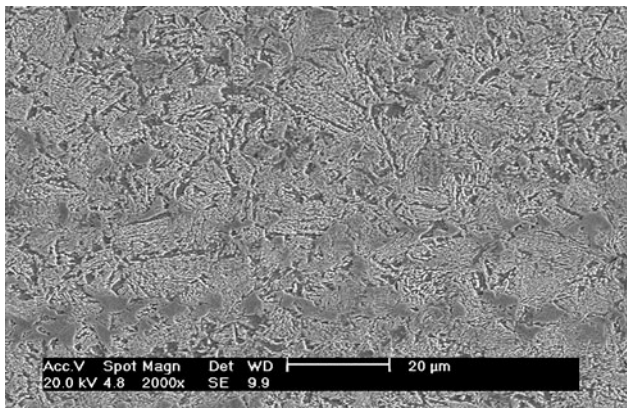
**Fig. 4** Jominy samples micrographics of SAE-6150 steel for regions located at different distances from the quenched surface: (a) 11.11 mm, 2000X, (b) 15.87 mm, 2000X, (c) 22.22 mm, 2000X, (d) 34.92 mm, 2000X and (e) 41.27 mm, 2000X

ture of martensite increases the relevance of domain rotation as a magnetization reversal mechanism. Domain rotation generates low MBN, as previously discussed [8, 32].

Figures 5 and 6 present the envelopes of the MBN signals measured in different positions for SAE 4140 and SAE 6150 samples, respectively. In order to avoid edge effects in



(d)



(e)

**Fig. 4** (Continued)

magnetic measurements, the first point, located at 9.52 mm was not considered in measurements.

In Figs. 5 and 6, the following aspects should be noticed:

- The MBN amplitude envelope is low in material regions next to the quenched surface, and increases gradually as this distance increases. These variations are caused by the changing microstructural constituents along the sample. In regions next to the quenched surface, a martensitic microstructure was observed, leading to significant domain rotation. With increasing distance from the quenched surface, cooling rate reduces and microstructure changes, presenting less martensite, and increasing bainite and other two phase (ferrite and cementite) eutectoid constituents. Presence of alpha-iron (also called ferrite) allows free domain wall movement, leading to higher MBN levels. This behavior has been found for both materials for the three excitation frequencies tested.
- The position of the MBN envelope peak was shifted from relatively high values of applied current to low ones, so that sample measurement points moved away from the quenched surface. All studied cases presented similar behavior. Martensitic microstructure, as produced next to the WJ surface, is magnetically very hard, and only with

high fields there is emission of MBN. Additionally, microstructures such as bainite (ferrite laths surrounded by coarse particles of cementite), generated in regions far from the WJ surface, produce MBN emissions for lower magnetic fields than those observed for martensite, which is agreement with reports of Kaplan et al. [31] and Kinser et al. [34].

- By increasing the excitation frequency, the positions of all envelope peaks move to lower values of applied current: the MBN envelope peak position is directly related to the position of the coercive field  $H_c$ , as shown by Jiles [35]. Also, by increasing the excitation frequency, eddy currents increase, which generates magnetic fields reacting to the external field. Therefore, the  $H_c$  value tends to increase with frequency, since the applied magnetic field is high enough for the magnetic saturation be attained, as discussed by Szczyglowski [36] and Chwastek et al. [37]. However, if the applied field is not sufficient for the magnetic saturation, this trend may not be observed. It should be noted that, for low frequency values, the effect of eddy currents is small and the dynamic movement of domain walls is especially important in the displacement of  $H_c$  values. Increasing the frequency, the number of active domain walls increases [38–40], affecting the dynamic hysteresis.

When MBN signals for both steels, are compared at the same distances to WJ surface, the 4140 steel MBN is always larger for all tested frequencies (Figs. 5 and 6). One factor that may have generated these differences can be represented by the coarse structures such as bainite constituted by ferrite laths surrounded by cementite. Ferrite laths also occur at longer distances from each other, which helps to increase MBN pulses. For example, taking a 22.22 mm distance from the WJ surface, the volumetric fraction of bainite for 6150 steel is smaller than that for 4140 steel. These data indicate possibility that the formation of bainite and its corresponding volumetric fraction (generated by the alloys elements concentrations in the steels) could be detected using the MBN test. Nonetheless, further studies should be performed by analyzing the joint presence of other factors that may influence the RMB behavior, especially the residual stresses effect.

Figures 7 and 8 show the distribution of several MBN parameters, over the length of SAE 4140 and SAE 6150 Jominy samples, for 5, 10 and 20 Hz frequencies. These MBN parameters are peak position, peak height and MBN-rms. In addition, HRC hardness measurement distributions for both materials are also presented.

MBN measurements confirm the metallographic analyses. Data collected for SAE-4140 and SAE-5160 Jominy samples indicate high hardness, 52 HRC and 55 HRC, in the martensitic region next to the quenched surface, and low

**Fig. 5** MBN profiles from different positions of SAE-4140 sample using 5, 10 and 20 Hz excitation frequencies

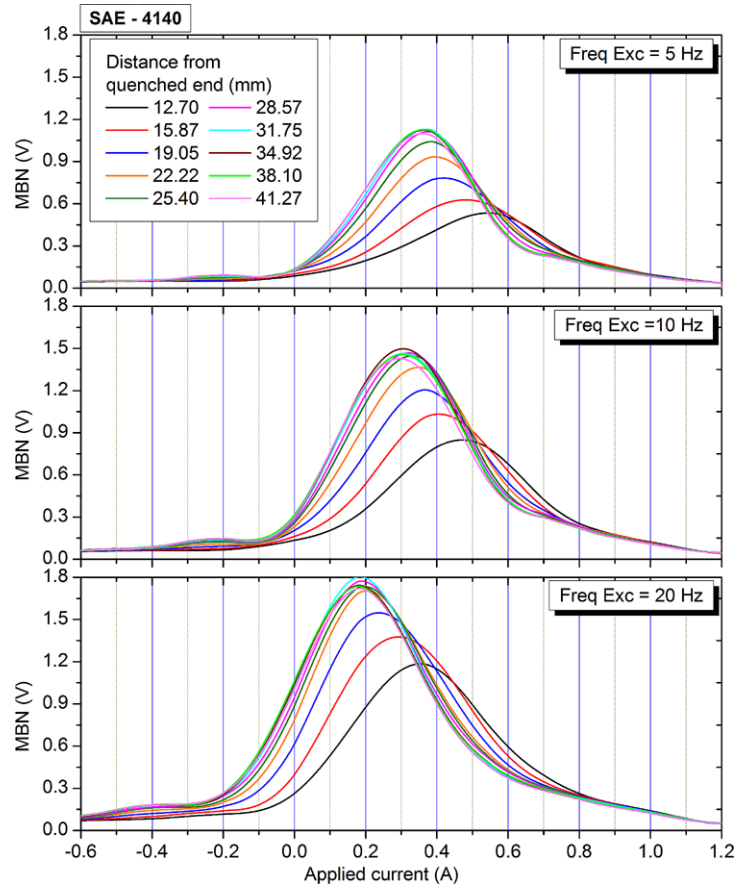


**Fig. 6** MBN profiles from different positions of SAE-6150 sample using 5, 10 and 20 Hz excitation frequencies

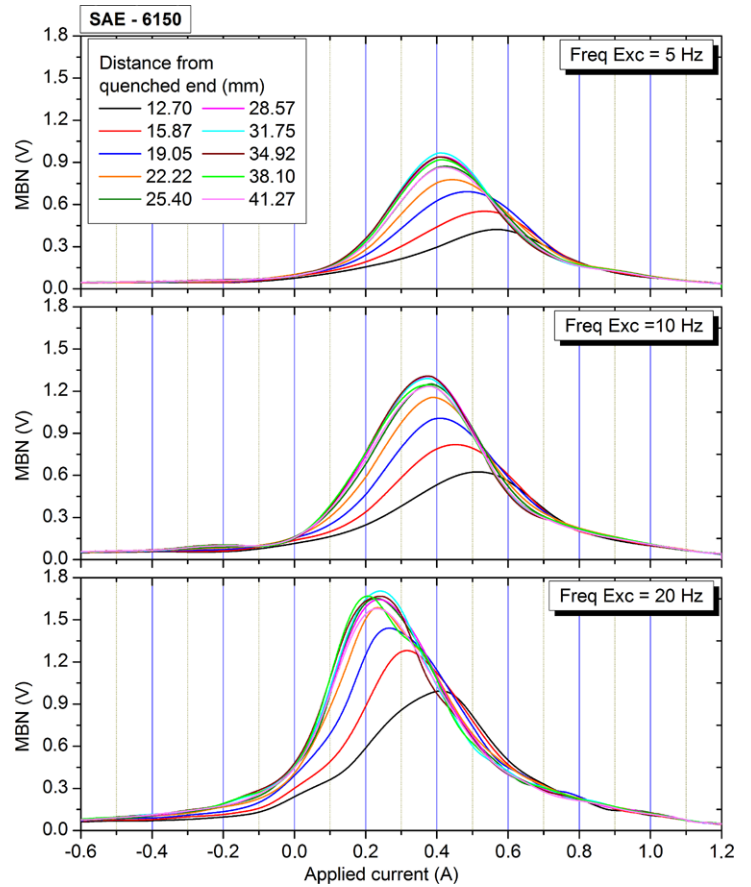




**Fig. 7** Distribution of different MBN parameters (peak position, peak height, rms) and hardness (HRC) measurements over the length of the SAE 4140 Jominy sample, obtained 5, 10 and 20 Hz excitation frequencies

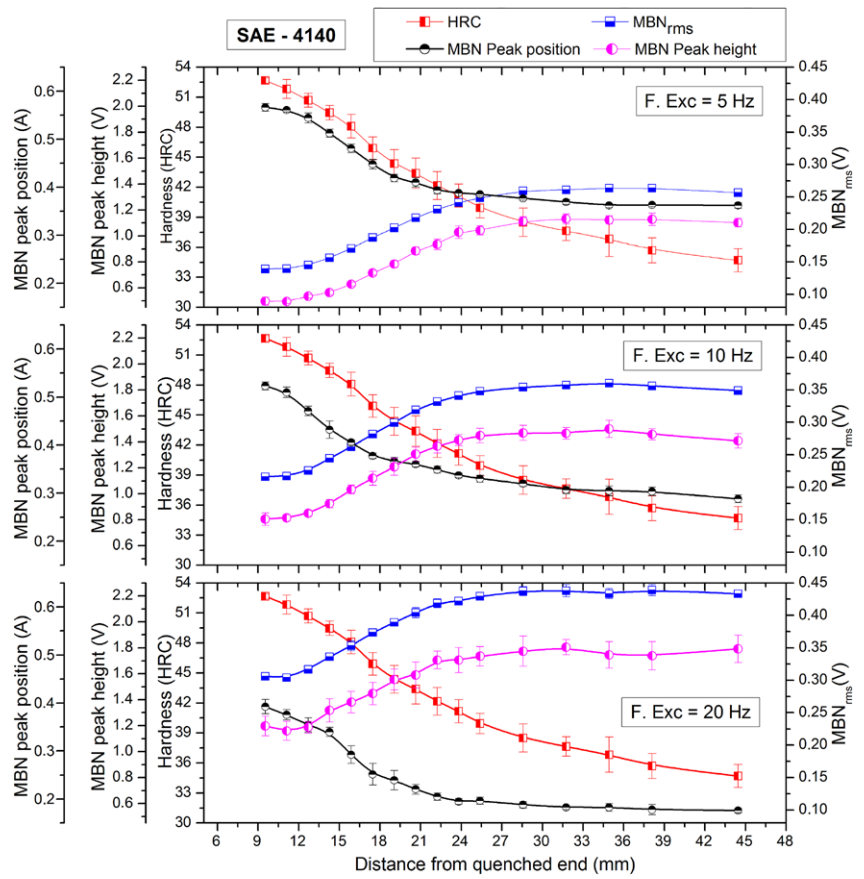


**Fig. 8** Distribution of different MBN parameters (peak position, peak height, rms) and hardness (HRC) measurements over the length of the SAE 6150 Jominy sample, obtained at 5, 10 and 20 Hz excitation frequencies

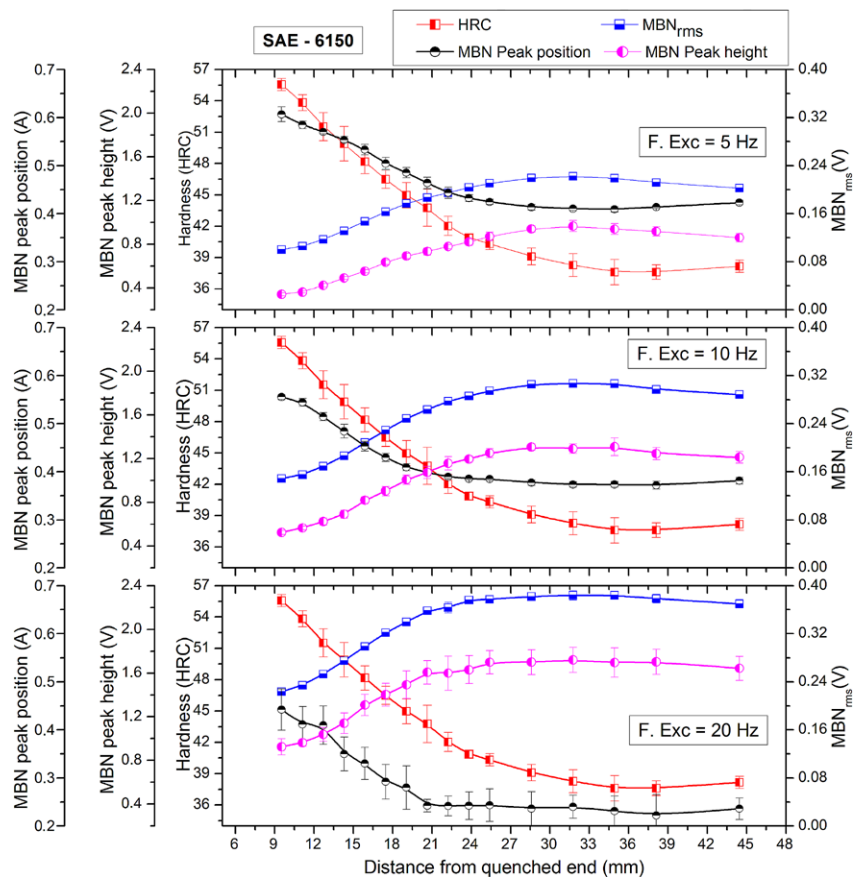
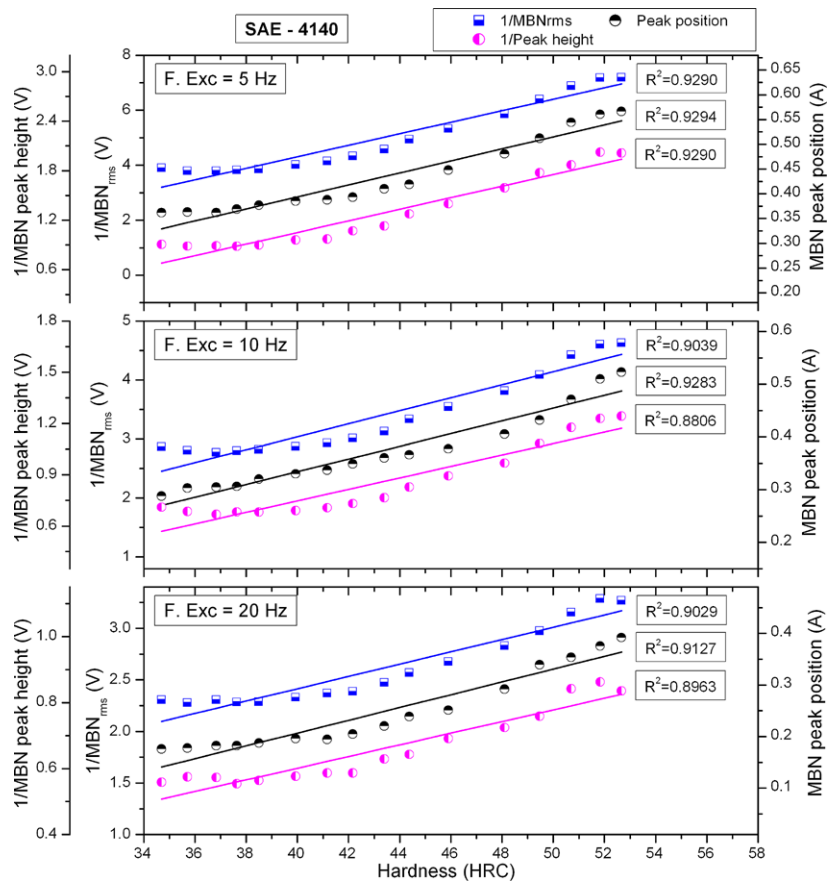


**Fig. 9** Dependence of different MBN parameters (peak position, 1/peak height, 1/MBNrms) on hardness (HRC) for SAE 4140 obtained at 5, 10 and 20 Hz excitation frequencies



hardness, 34 HRC and 38 HRC, in regions far away from the quenched surface (bainite and other constituents).

Similarly, when measurement points are far away from the quenched surface, values of HRC hardness measurements and of MBN peak position decrease, whereas MBN peak height and MBNrms parameters increase. All graphs show the profile change that accompanies microstructural variations caused by heat treatment. This phenomenon is observed in both SAE-4140 and SAE-6150 steels.

In regions next to the quenched surface, the microstructure presents large amounts of martensite. The small martensite needles, as well as the stressed lattice full of crystalline defects originated by the martensitic transformation, make difficult magnetic domain wall movement. Besides, the fine microstructure enables domain rotation as a reversal mechanism instead of domain wall movement [8, 32]. These conditions limit MBN emissions, and then peak height and MBNrms parameters show low amplitudes. Therefore, reversal of magnetization requires strong fields, and the MBN peak positions are situated at relatively high magnetic fields when there is martensite [28].

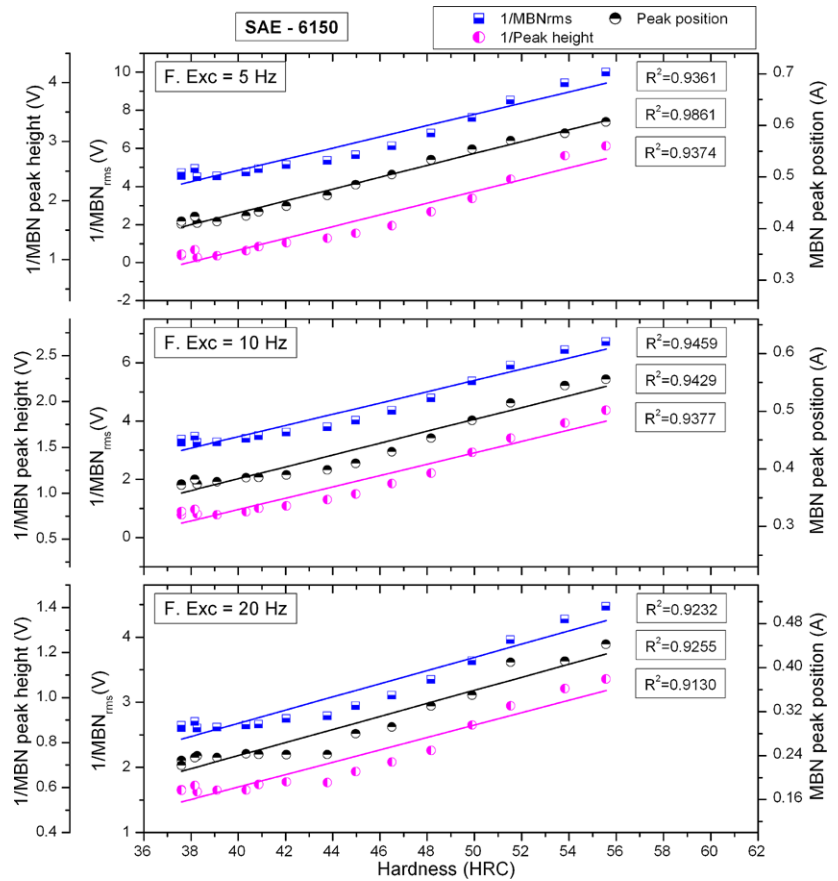
With the reduction of cooling rates at greater distances from the quenched surface, the microstructure gradually changes with decreasing lattice defect density and martensite volumetric fraction. At the same time, the amount of

bainite and other constituents formed after decomposition of austenite increase. For a region located at 41.27 mm from the quenched surface, the microstructure presents reduced content of martensite. Therefore, domain wall movements became easier. In this condition, MBN emissions rise (e.g., peak height and MBNrms increase) and the field amplitude necessary to reverse magnetization falls (MBN peak position decreases).

The relationship between hardness and different MBN parameters (peak position, 1/peak height, 1/MBNrms) acquired with 5, 10 and 20 Hz excitation frequencies is shown in Figs. 9 and 10, for SAE-4140 and SAE-5160 samples, respectively.

The graphs of Figs. 9 and 10 demonstrate the existence of good linear correlations between all MBN parameters and hardness. As seen in Figs. 7–10, Peak Position is the MBN parameter presenting the best correlation. An increase in excitation frequency causes reduction of R<sup>2</sup> linear correlation indexes for all calculated parameters. The amount of registered pulses decreases and the MBN increases with the rise of excitation frequency, which was also reported by Mitra and Jiles [41], Pala and Bydzovsky [42] and Stupakov et al. [43]. Thus, the reduction produced by increasing the excitation frequency, in the calculated linear correlation coefficient

**Fig. 10** Dependence of different MBN parameters (peak position, 1/peak height, 1/MBNrms) on hardness (HRC) for SAE 6150 obtained at excitation frequencies of 5, 10 and 20 Hz



icients, can be attributed to the decreasing number of registered pulses.

#### 4 Conclusions

Measurements of Magnetic Barkhausen Noise have been carried out to characterize the microstructure of a Jominy test performed with SAE-4140 and SAE-6150 samples. Microstructures and values of hardness were obtained for different regions by a destructive conventional test. Different MBN parameters were calculated and compared with hardness measurement and microstructure analysis. The following conclusions can be drawn:

Metallographic analyses of samples, for both tested materials, present continuous microstructure variation with different density of crystal defects along the measured surface, which was submitted to different cooling rates. Insofar as the cooling rate decreases, microstructure continuously changed from martensite to bainite and other coarser microstructural constituents.

For the investigated Jominy test samples, the calculated MBN signal parameters follow the cooling gradient. There are linear correlations between different MBN parameters and hardness measurements.

Increasing excitation frequency (5 Hz to 20 Hz) slightly diminishes linear correlation coefficients between different calculated MBN parameters and hardness amplitudes. This effect increased with excitation frequency, thus reducing the sensitivity of the technique.

Formations of coarser structures, such as bainite composed by ferrite laths surrounded by cementite can increase MBN pulses, possibly because the ferrite laths are more separated from each other. The data suggest the possibility of determination of the volumetric fraction of microstructural constituents such as bainite by using the MBN test. Nonetheless, further studies should be performed by analyzing the joint presence of other factors that also influence the RMB behavior, for example the residual stresses.

**Acknowledgements** The authors would like to thank the State of São Paulo Research Foundation, FAPESP (Process 05/57146-0). M.F. de Campos and L.R. Padovese thank CNPq. We thank Dr. Martin Sablik for the critical reading of the manuscript.

#### References

- Hosford, W.F.: Physical Metallurgy. Taylor & Francis, London (2005)
- Fong, H.S.: Further observations on the Jominy end quench test. *J. Mater. Process. Technol.* **38**(1–2), 221–225 (1993)

3. Zehtab Yazdi, A., Sajjadi, S.A., Zebarjad, S.M., Moosavi Nezhad, S.M.: Prediction of hardness at different points of Jominy specimen using quench factor analysis method. *J. Mater. Process. Technol.* **199**, 124–129 (2008)
4. Vermeulen, W.G., Van der Wolk, P.J., Weijer, A.P., van der Zwaag, S.: Prediction of Jominy hardness profiles of steels using artificial neural networks. *J. Mater. Eng. Perform.* **5**(1), 57–63 (1996)
5. Overshott, K.J.: Magnetism: it is permanent. *IEE Proc. A* **138**(1), 22–30 (1991)
6. Costa, L.F.T., Giroto, F., Baiotto, R., Gerhardt, G., de Campos, M.F., Missell, F.P.: Influence of microstructural constituents on the hysteresis curves in 0.2%C and 0.45%C steels. *J. Phys. Conf. Ser.* **303**, 012029 (2011)
7. Barkhausen, H.: Two with help of new repeating rediscovered appearances by H. Barkhausen—the silence during unmagnetising of iron. *Phys. Z.* **20**, 401–403 (1919)
8. Monlevade, E.F., de Campos, M.F., Franco, F.A., Capo-Sanchez, J., Goldenstein, H., Padovese, L.R.: Magnetic Barkhausen noise in quenched carburized nickel-steels. *IEEE Trans. Magn.* **48**, 1465–1468 (2012)
9. ASM Handbook, vol. 4: Heat Treating, 10th edn. (1991)
10. de Campos, M.F., Campos, M.A., Landgraf, F.J.G., Padovese, L.R.: Anisotropy study of grain oriented steels with magnetic Barkhausen noise. *J. Phys. Conf. Ser.* **303**, 012020 (2011)
11. Hwang, D.G., Kim, H.C.: The influence of plastic deformation on Barkhausen effects and magnetic properties in mild steel. *J. Phys. D, Appl. Phys.* **21**, 1807–1813 (1988)
12. O’Sullivan, D., Cotterell, M., Tanner, D.A., Meszaros, I.: Characterisation of ferritic stainless steel by Barkhausen techniques. *Nondestruct. Test. Eval. Int.* **37**, 489–496 (2004)
13. Capó Sánchez, J., de Campos, M.F., Padovese, L.R.: Magnetic Barkhausen emission in lightly deformed AISI 1070 steel. *J. Magn. Magn. Mater.* **324**, 11–14 (2012)
14. Moorthy, V., Shaw, B.A., Mountford, P., Hopkins, P.: Magnetic Barkhausen emission technique for evaluation of residual stress alteration by grinding in case-carburised En36 steel. *Acta Mater.* **53**, 4997–5006 (2005)
15. Gauthier, J., Krause, T.W., Atherton, D.L.: Measurement of residual stress in steel using the magnetic Barkhausen noise technique. *Nondestruct. Test. Eval. Int.* **31**, 23–31 (1998)
16. Altpeter, I., Dobmann, G., Kroning, M., Rabung, M., Szielasko, S.: Micro-magnetic evaluation of micro residual stresses of the IInd and IIIrd order. *Nondestruct. Test. Eval. Int.* **42**, 283–290 (2009)
17. Hauk, V.: *Structural and Residual Stress Analysis by Nondestructive Methods*. Elsevier Science, Amsterdam (1997)
18. de Campos, M.F., Sablik, M.J., Landgraf, F.J.G., Hirsch, T.K., Machado, R., Magnabosco, R., Gutierrez, J., Bandyopadhyay, A.: Effect of rolling on the residual stresses and magnetic properties of a 0.5 % Si electrical steel. *J. Magn. Magn. Mater.* **320**, e377–e380 (2008)
19. Lindgren, M., Lepisto, T.: Effect of cyclic deformation on Barkhausen noise in mild steel. *Nondestruct. Test. Eval. Int.* **36**, 401–409 (2003)
20. Meyendorf, N., Roesner, H.: Depth profiling of machined surfaces using cross correlation of Barkhausen noise butterfly curves. In: Thompson, D.O., Chimenti, D.E. (eds.) *Review of Quantitative Nondestructive Evaluation*, vol. 22, pp. 1697–1704. American Institute of Physics, New York (2003)
21. Capo-Sanchez, J., Perez-Benitez, J., Padovese, L.R.: Analysis of the stress dependent magnetic easy axis in ASTM 36 steel by the magnetic Barkhausen noise. *Nondestruct. Test. Eval. Int.* **40**, 168–172 (2007)
22. Stefanita, C.G., Atherton, D.L., Clapham, L.: Plastic versus elastic deformation effects on magnetic Barkhausen noise in steel. *Acta Mater.* **48**, 3545–3551 (2000)
23. Alberteris Campos, M., Capo-Sanchez, J., Benitez, J.P., Padovese, L.R.: Characterization of the elastic-plastic region in AISI/SAE 1070 steel by the magnetic Barkhausen noise. *Nondestruct. Test. Eval. Int.* **41**, 656–659 (2008)
24. Anglada-Rivera, J., Padovese, L.R., Capo-Sanchez, J.: Magnetic Barkhausen noise and hysteresis loop in commercial carbon steel: influence of applied tensile stress and grain size. *J. Magn. Magn. Mater.* **231**, 299–306 (2001)
25. Moorthy, V., Shaw, B.A., Hopkins, P.: Magnetic Barkhausen emission technique for detecting the overstressing during bending fatigue in case-carburised En36 steel. *Nondestruct. Test. Eval. Int.* **38**, 159–166 (2005)
26. Palma, E.S., Mansur, T.R., Silva, S.F., Alvarenga, A.: Fatigue damage assessment in AISI 8620 steel using Barkhausen noise. *Int. J. Fatigue* **27**, 659–665 (2005)
27. Altpeter, I.: Nondestructive evaluation of cementite content in steel and white cast iron using inductive Barkhausen noise. *J. Nondestruct. Eval.* **15**, 45–60 (1996)
28. Gur, C.H., Cam, I.: Comparison of magnetic Barkhausen noise and ultrasonic velocity measurements for microstructure evaluation of SAE 1040 and SAE 4140 steels. *Mater. Charact.* **58**, 447–454 (2007)
29. Davut, K., Gur, C.H.: Monitoring the microstructural changes during tempering of quenched SAE 5140 steel by magnetic Barkhausen noise. *J. Nondestruct. Eval.* **26**, 107–113 (2007)
30. Kleber, X., Hug, A., Merlin, J., Soler, M.: Ferrite-martensite steels characterization using magnetic Barkhausen noise measurements. *ISIJ Int.* **44**, 1033–1039 (2004)
31. Kaplan, M., Gur, C.H., Erdogan, M.: Characterization of dual-phase steels using magnetic Barkhausen noise technique. *J. Nondestruct. Eval.* **26**, 79–87 (2007)
32. de Campos, M.F., Franco, F.A., Santos, R., Silva, F.S., Ribeiro, S.B., Lins, J.F.C., Padovese, L.R.: Magnetic Barkhausen noise in quenched carburized steels. *J. Phys. Conf. Ser.* **303**, 012030 (2011)
33. ASTM-A225: Standard Test Methods for Determining Hardenability of Steel. ASTM Standards (1999)
34. Kinser, E.R., Lo, C.C.H., Barsic, A.J., Jiles, D.C.: Modeling microstructural effects on Barkhausen emission in surface-modified magnetic materials. *IEEE Trans. Magn.* **41**, 3292–3294 (2005)
35. Jiles, D.C.: Dynamics of domain magnetization and the Barkhausen effect. *Czechoslov. J. Phys.* **50**, 893–924 (2000)
36. Szczygłowski, J.: Influence of eddy currents on magnetic hysteresis loops in soft magnetic materials. *J. Magn. Magn. Mater.* **223**, 97–102 (2001)
37. Chwastek, K., Szczygłowski, J., Najgebauer, M.: A direct search algorithm for estimation of Jiles–Atherton hysteresis model parameters. *Mater. Sci. Eng. B* **131**, 22–26 (2006)
38. de Campos, M.F., Teixeira, J.C., Landgraf, F.J.G.: The optimum grain size for minimizing the energy losses in iron. *J. Magn. Magn. Mater.* **301**, 94–99 (2006)
39. Haller, T.R., Kramer, J.J.: Observation of dynamic domain size variation in a silicon-iron alloy. *J. Appl. Phys.* **41**, 1034–1035 (1970)
40. Haller, T.R., Kramer, J.J.: Model for reverse-domain nucleation in ferromagnetic conductors. *J. Appl. Phys.* **41**, 1036–1037 (1970)
41. Mitra, A., Jiles, D.C.: Magnetic Barkhausen emissions in as-quenched Fe-Si-B amorphous alloy. *J. Magn. Magn. Mater.* **168**, 169–176 (1997)
42. Pala, J., Bydzovsky, J.: Dependence of Barkhausen noise in plastically deformed steel on frequency and nonlinearity of magnetizing field. *Acta Phys. Pol. A* **113**, 23–26 (2008)
43. Stupakov, O., Pala, J., Takagi, T., Uchimoto, T.: Governing conditions of repeatable Barkhausen noise response. *J. Magn. Magn. Mater.* **321**, 2956–2962 (2009)